A BIOMECHANICAL MODEL FOR THE ANALYSIS OF THE CERVICAL SPINE IN STATIC POSTURES

C. J. Snijders,* G. A. Hoek van Dijke,* and E. R. Roosch†

*Faculty of Medicine, Department of Biomedical Physics and Technology, Erasmus University, Rotterdam; and †Surgeon General's Office, Royal Netherlands Airforce, Soesterberg, The Netherlands

Abstract—To gain a better understanding of the forces working on the cervical spine, a spatial biomechanical computer model was developed. The first part of our research was concerned with the development of a kinematic model to establish the axes of rotation and the mutual position of the head and vertebrae with regard to flexion, extension, lateroflexion and torsion. The next step was the introduction of lines of action of muscle forces and an external load, created by gravity and accelerations in different directions, working on the centre of gravity of the head and possibly a helmet. Although the results of our calculations should be interpreted cautiously in the present stage of our research, some conclusions can be drawn with respect to different head positions. During flexion muscle forces and joint reaction forces increase, except the force between the odontoid and the ligamentum transversum atlantis. This force shows a minimum during moderate flexion. The joint reaction forces on the levels C_0–C_1, C_1–C_2, and C_7–T_1 reach minimum values during extension, each in different stages of extension. Axial rotation less than 35° does not need great muscle forces, axial rotation further than 35° causes muscle forces and joint reaction forces to increase fast. While performing, lateral flexion muscle forces and joint reaction forces must increase rapidly to balance the head. We obtained some indications that the order of magnitude of the calculated forces is correct.

1. INTRODUCTION

In high performance aircraft complicated situations arise with regard to the cervical spine under load, e.g. when sudden accelerations occur while the pilot is looking backwards. As far as the spine is concerned, most research is devoted to the lumbar area (Schulz *et al.*, 1982a, b; Shirazi-Adl *et al.*, 1986; Miller *et al.*, 1986). Less research has been done on the cervical spine (Rizzi and Covelli, 1975a, b; Less and Eickelberg, 1976; Penning, 1978; Kazarian *et al.*, 1979; Rieck, 1981; Dul *et al.*, 1982; Glaister, 1987; McElhaney *et al.*, 1989), which gives us little kinematic and anthropometric data. So far, interest has been focused on helmet design and helmet mounted devices (Petrofsky and Phillips, 1982; Phillips and Petrofsky, 1983). The lack of previous studies should be taken into account when considering this study. De Graef and Ingels (1982) and Aghina (1984) studied cervical complaints in the case of F-16 pilots and concluded that the origin of discomfort and fatigue was closely related to the degree and duration of the 'vertical' acceleration (A_z-acceleration). The weight of the helmet, the position of the head and the fatigue of the aviator also play an important role. Little attention is paid to these aspects in medical literature on aerospace. Most studies deal with the origin of acute trauma caused by unexpected movements of the aircraft and the use of an ejection seat. Experimental research has also been done on maximal sustainable forces in the neck.

A study was initiated by the Royal Netherlands Airforce Surgeon General's Office to analyse the load on neck structures under various levels of G-load. This paper presents the biomechanical model which was introduced to enable the calculation of the forces in a number of neck muscles and in the joints of the cervical spine. The distribution of forces in a specific joint has not been analysed. This model is used to analyse a number of flight situations, the results of these investigations will be presented in a second paper.

2. BIOMECHANICAL MODEL

2.1. Kinematic model

The head and the neck form a kinematic chain consisting of eight links. Each link has six degrees of freedom. The connecting joints restrict the degrees of freedom and the amount of motion. The upper cervical spine consists of the atlas and the axis which form a loose connection which means that muscular forces are always needed for the positioning and stability of the head. The vertebrae C_3–C_7 possess intervertebral discs.

The first simplification of the model is the assumption that the axes of rotation are located in the middle of the respective joints. Furthermore, the vertebrae C_3–C_7 are not modelled as separate units. The intervertebral discs and the interwoven muscles cause this part of the cervical spine to function as a unit (Penning, 1978). This allows for the vertebrae C_3–C_7 to be regarded as one link. The variable distance between C_2 and C_7 during bending and stretching of the cervical spine is incorporated into the model by means of a variable length of this link. Intrinsic forces in this part of the spine are not incorporated into the model.

BM 24:9-A

Figure 1 shows the model in the neutral position in the sagittal plane. Flexion/extension is possible in the points B, C, E and O. B is the centre of rotation of the atlanto occipital joint in the sagittal plane, the angle in this joint is called λ. μ is the angle between the atlas and the axis with C as the centre of rotation, v is the angle between the axis and C_3 in point E. The origin O of the coordinate system is on the caudal-dorsal corner of the vertebra C_7, this is the centre of rotation of the link OE. The length of the link OE is variable, depending on the angle φ representing the inclination of this link.

The point TC is situated at the top of the clivus, corresponding with the location of the centre of gravity of the head. PO is the point of attachment of the dorsal neck muscles at the protuberance occipitalis. The angle of the head with respect to the movement in the sagittal plane is called β. The configuration of joints in Fig. 1 represents the neutral position of the head: when the person is looking in the forward direction while his direction of view and the horizontal plane meet at an angle of 15°, β is zero in the neutral position. Appendix A contains a complete list of all points incorporated into the model. The dimensions of parameters were found in the literature (White and Panjabi, 1978; Dul *et al.*, 1982) or estimated on the basis of X-ray photographs.

Figure 2a shows a frontal view of the model in lateroflexion, the axes of rotation for lateroflexion are shown in Fig. 2b. The axis a_1 for lateral flexion in the atlanto occipital joint is situated in point A, at a distance of 17 mm from point B. The direction of this axis is horizontal in the neutral position. The angle between the head and the atlas is called θ_1. θ_2 is the angle between the axis and C_3, point E is the centre of lateral flexion at this level. The axis of rotation a_2 is the bisector of the angle OED. The link OE is able to
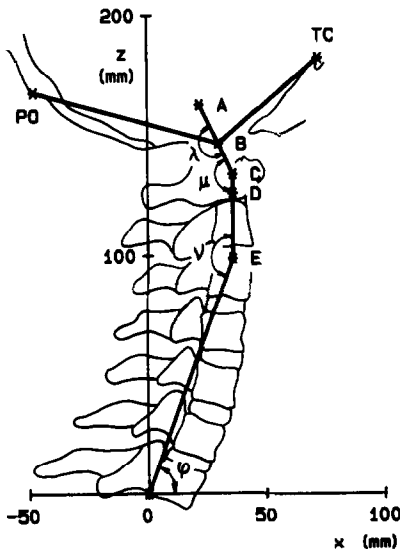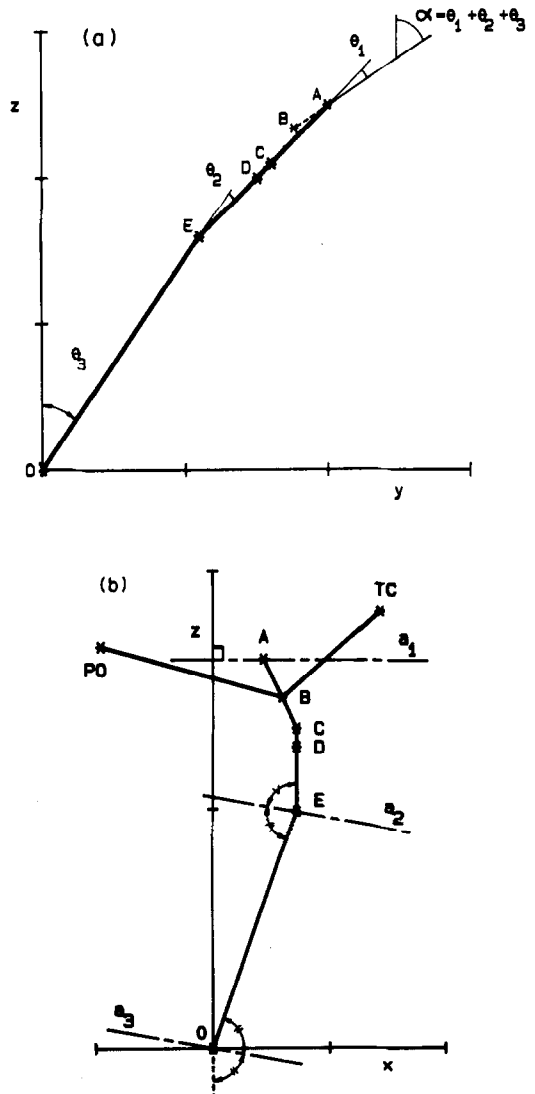
Fig. 2. (a) Front view of the kinematic model in lateroflexion (graph not to scale). (b) Axes of rotation for lateroflexion.

perform lateral flexion on point O on an axis a_3 which coincides with the bisector of the angle between OE and the negative part of the z-axis. The angle of this rotation is called θ_3. No lateral flexion is assumed to take place on C_1–C_2. The angle of the head with respect to the movement in the frontal plane is called α.

The axial rotation γ of the head is the result of the contributions ρ_1 on the level C_1–C_2 and ρ_2, spread over C_3–C_7. The centre of rotation for ρ_1 is the odontoid, represented by point D, 8 mm below point C. The spread rotation over C_3–C_7 is represented as a single rotation on OE.

The next part of the kinematic model deals with the relations between the head and the respective vertebrae. The location of points in the neutral position and the relations for forward flexion are based on anthropometric data valid for an average adult man

Fig. 1. Side-view of the kinematic model, neutral position. Ventral side is at the right.

(Dul et al., 1982). For other movements the relations are based on the proportions of the limits of motion of the respective joints (White and Panjabi, 1978).

2.1.1. *Forward flexion.* A distinction is made between the stages knicking in C_0–C_1 during the first 8° of rotation, and buckling and bending of C_1–C_2, C_2–C_3 and C_3–C_7, for angles between 8 and 45°. In this phase C_0–C_1 shows a relative retroflexion from $+8$ to $-8°$. So for these stages of flexion the following algorithms were assumed in the kinematic model:

$0 \leqslant \beta \leqslant 8°$: $\Delta\lambda = \beta$

$\Delta\mu = \Delta\nu = \Delta\varphi = 0,$

$8 \leqslant \beta \leqslant 45°$: $\Delta\lambda = 8° - (16/37) * (\beta - 8)°$

$\Delta\mu = \quad (\ 8/37) * (\beta - 8°)$

$\Delta\nu = \quad (20/37) * (\beta - 8)°$

$\Delta\varphi = \quad -(25/37) * (\beta - 8)°.$

(N.B.: The angles λ, μ, ν and φ have initial values which describe the neutral position, shown in Fig. 1. In this position the angles α, β and γ are zero. The angles $\Delta\lambda$, $\Delta\mu$, $\Delta\nu$ and $\Delta\varphi$ are changes with respect to the neutral position.) Due to the decreasing lordosis of the cervical spine while rotating the head forward, the distance between O and E increases. In the literature (Dul et al., 1982), the length of the link OE was found only for $0 \leqslant \beta \leqslant 8°$ (OE_1) and for $\beta = 45°$ (OE_2). The length OE of this link is calculated by linear interpolation between these values:

$0 \leqslant \beta \leqslant 8°$: $OE = OE_1$

$8 \leqslant \beta \leqslant 45°$: $OE = OE_1 + \dfrac{(OE_2 - OE_1)}{37} * (\beta - 8)°.$

2.1.2. *Backward flexion.*

$-89° \leqslant \beta \leqslant 0°$: $\Delta\lambda = (13/89) * \beta$

$\Delta\mu = (10/89) * \beta$

$\Delta\nu = (33/89) * \beta$

$\Delta\varphi = (33/89) * \beta.$

No data are available about the distance between the points O and E, so the same relationship as for forward flexion is assumed:

$$OE = OE_1 + \frac{(OE_2 - OE_1)}{37} * (\beta)°.$$

No substantial influence is expected by the simplification of linear interpolation between $\beta = 8$ and 45°, because the lengthening of OE concerns only 5 mm from 105 mm (OE_1) to 110 mm (OE_2). Additional research is needed to validate the algorithm for $\beta \leqslant 0°$.

2.1.3. *Lateral flexion.* The relations between θ_1, θ_2 and θ_3 are given by:

$$\theta_1 = (\ 8/55) * \alpha$$
$$\theta_2 = (10/55) * \alpha$$
$$\theta_3 = (37/55) * \alpha.$$

A positive value of α refers to lateroflexion to the left.

2.1.4. *Axial rotation.* The angles ρ_1 and ρ_2 are computed as follows:

$$\rho_1 = (47/98) * \gamma$$
$$\rho_2 = (51/98) * \gamma.$$

A positive value of β refers to axial rotation to the left.
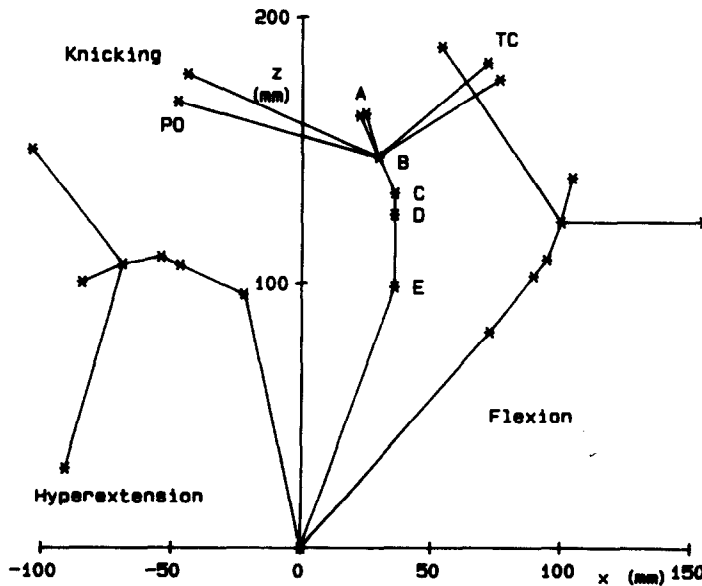

Fig. 3. Different stages of flexion/extension movement: hyperextension, knicking of the head and forward flexion. The first 8° from neutral position, the head knicks in C_{01}. The next phase between 8 and 45° knicking of the head, buckling of the atlas and bending of the lower cervical spine occur.

2.2. *Muscle forces*

The next step in biomechanical modelling was the introduction of the forces produced by the muscles. First, the muscles were selected that are supposed to make the largest contribution to the stabilization of the head and the neck. This selection was made on the basis of size and moment arm of the various muscles. The muscles which are incorporated into the model are listed in Appendix A. Next, the origin and insertion of each muscle had to be estimated, based on anatomy text books and anthropometric literature (Kiss and Szentágothai, 1964; von Lanz and Wachsmuth, 1955; Wells, 1971; Romanes, 1981).

Figure 4 shows a side view, a frontal view and a three-dimensional drawing of the link C_0. FTRL and

FTRR are the lines of action of the left and right trapezius muscle, respectively. The letters FSCML and FSCMR are short for left and right sternocleidomastoid muscle. FRC is the m. rectus capitus represented here by one line of action attached to the frontal side of the arc of the atlas, point C1V. The origin is located on the pars basilaris, point PB.

The input parameters for the model are the weight of the head and, if required, acceleration forces and the weight of a helmet. No friction is assumed in the joints, so the joint reaction force consists of three components (in x-, y- and z-directions). Basically, three muscle forces are sufficient to equilibrate the six degrees of freedom of the head. Due to the number of muscle forces (five muscle forces for the link C_0), the static
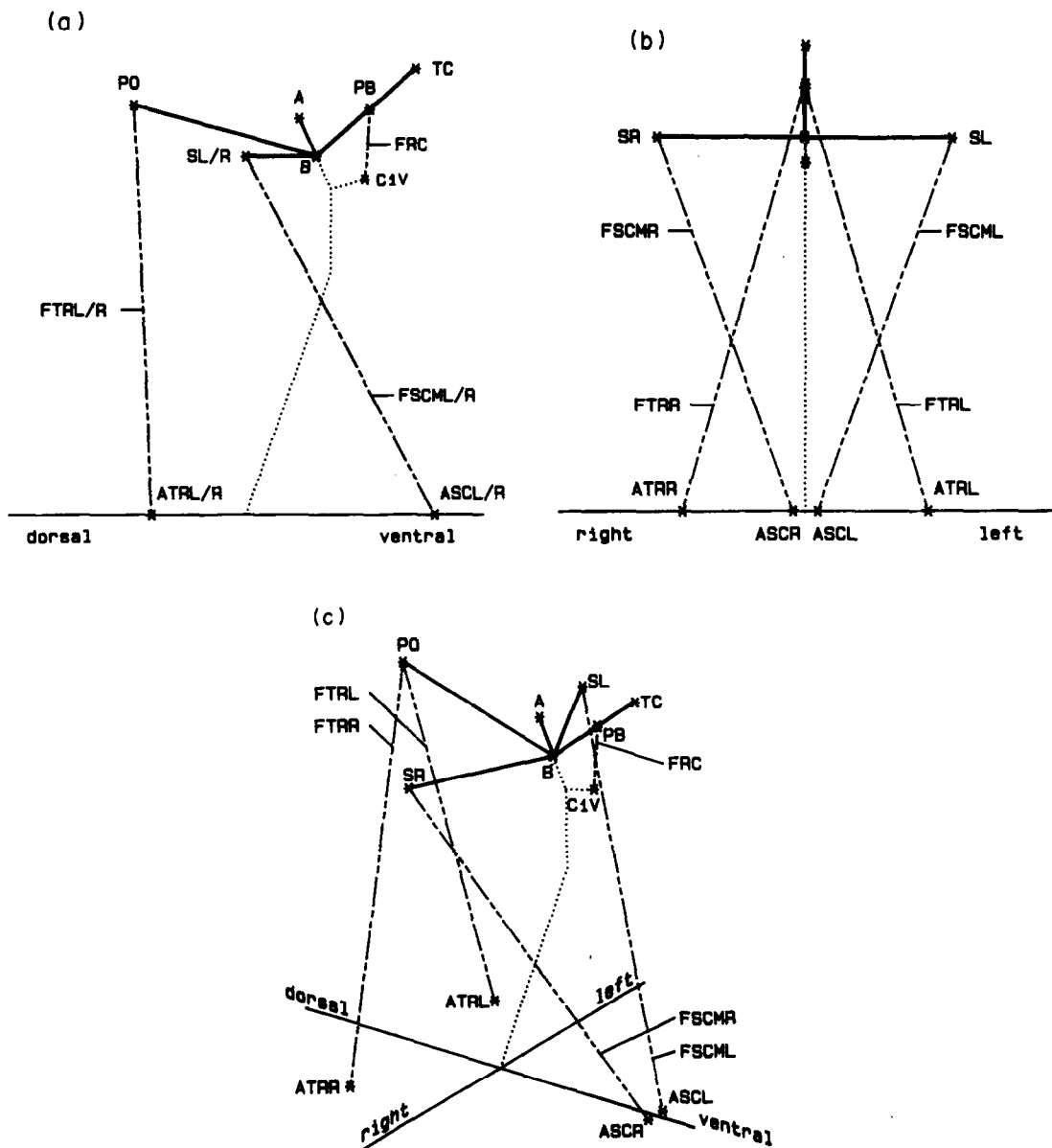

Fig. 4. Side view (a), front view (b) and three-dimensional drawing (c) of the link C_0. The dashed lines represent the lines of action of the muscles acting on this link.

model is overdetermined. Therefore, a basic optimization algorithm was used which calculates the muscle forces and joint reaction force for every combination of three muscles. Considering the restriction that muscles only can produce tension forces, the solution which led to the smallest joint reaction force in the atlanto occipital joint was chosen as the final solution (Schultz et al., 1982a, b). The choice for this criterion will be discussed later. From the calculation of the equilibrium of the head, the muscle forces and the total reaction force in the atlanto occipital joint were derived.

Next, the same procedure was followed to calculate the equilibrium of the atlas, with the atlanto occipital joint reaction force calculated above as an input parameter. The reaction force in the C_2–C_3 joint was input parameter for a similar procedure for the lower cervical spine. With regard to the equilibrium of the atlas, special attention was paid to the force in the ligamentum transversum atlantis. As shown in Fig. 5, the force between odontoid and ligament (FT) can become substantial when the person is bending forward.

The force and moment balance equations are presented in Appendix B.

3. RESULTS

With the help of the model muscle forces and joint reaction forces can be estimated. Figure 6 is the result of the calculation of the equilibrium of moments and
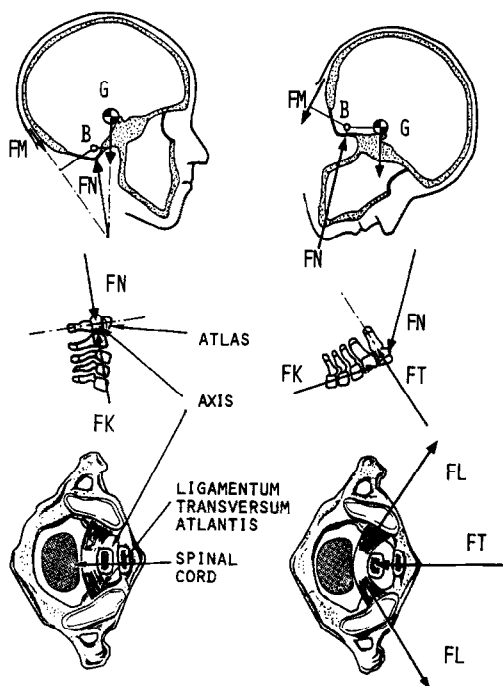
forces when the head is in the neutral position. Here, the only input parameter is the weight of the head, being 45 N (Williams and Lissner, 1962). In this position no muscle force is needed to equilibrate the atlas.

From the neutral position, calculations can be made for flexion, extension, lateroflexion, torsion and combinations of these different rotations. In Fig. 7a the joint reaction forces are shown as a function of flexion and extension, Fig. 7b shows the muscle forces. The muscle forces not shown in the graph are zero. For $\beta = -55°$ the centre of gravity of the head is above the atlanto occipital joint. In this situation no muscle force is needed to equilibriate the head, the joint reaction force FN reaches a minimum value. A similar situation occurs for $\beta = -30°$ for the link C_3–C_7: at this angle the load on this link is pointed at point O. During flexion and extension no muscle force is needed to balance the atlas. The forces FK and FT are sufficient to equilibriate the load FN.

The muscle forces, as predicted by the model, are just minimum forces to balance the links. There will also be muscle force for reasons of stability, this will be discussed later.

In Fig. 8a the joint reaction forces are calculated for the maximal excursion in axial rotation. Figure 8b shows the muscle forces acting on C_0, Fig. 8c the muscle forces on C_1 and Fig. 8d the muscle forces acting on C_3–C_7. While rotating the head, the centre of gravity stays at the ventral side of the atlanto occipital joint, so FRC is not necessary for the equilibrium of the head.

The graphs show a great difference between rotations less than 35° and rotations greater than 35°. Rotating the head less than 35° in a positive direction
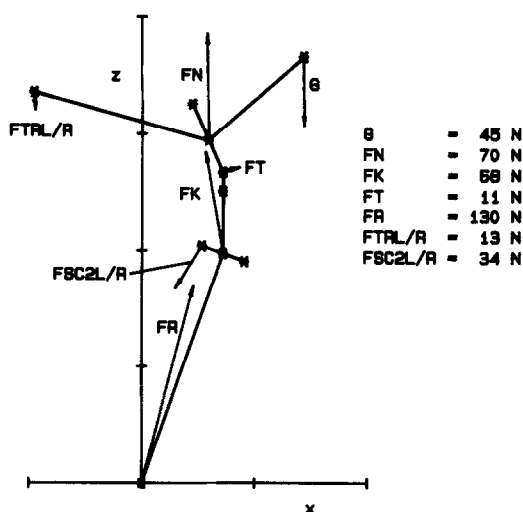

Fig. 5. Force FT in the ligamentum transversum atlantis arising from pressure of the odontoid, preventing shearing of the atlas on the axis.

Fig. 6. Forces in muscles and joints when the head is in the neutral position. FN is the joint reaction force in the atlanto occipital joint. FK in C_2–C_3 and FR in C_7–T_1. The forces are drawn acting from a caudal structure (muscle or condyle) on a cranial structure. The joint reaction forces are in the sagittal plane whereas the muscle forces are not.
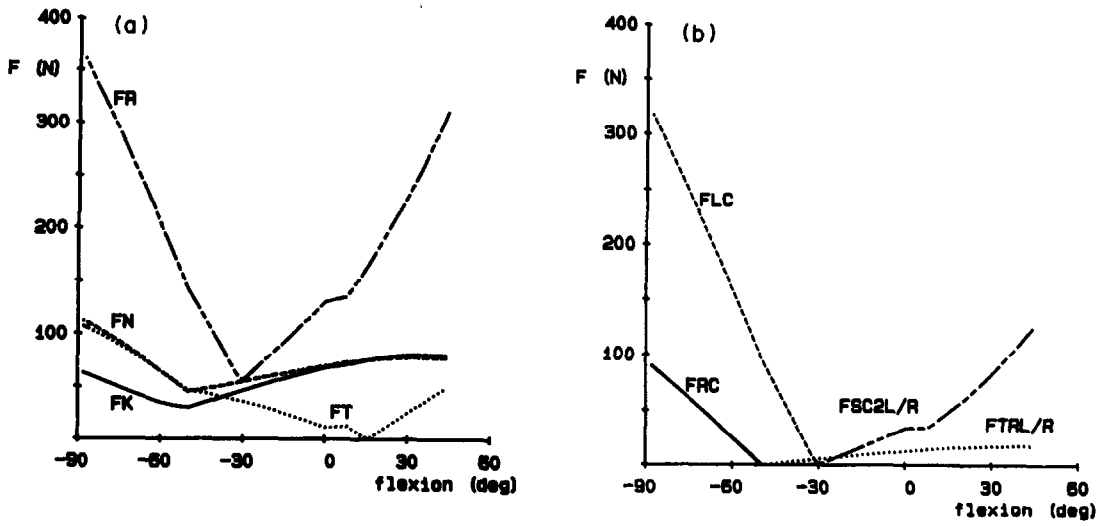
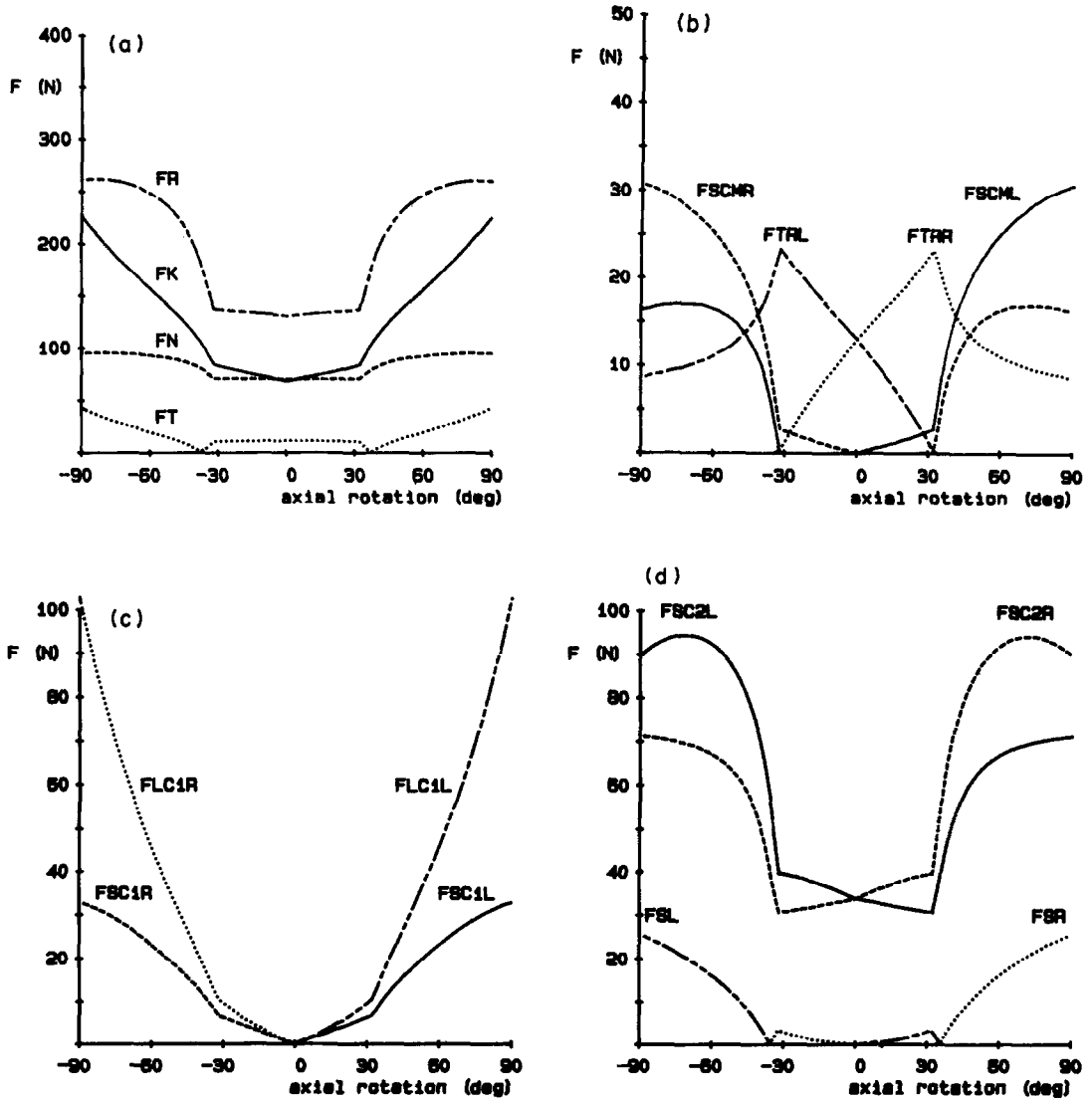Fig. 7a, b. Joint reaction forces and muscle forces as a function of flexion (β).

Fig. 8a, b, c, d. Joint reaction forces and muscle forces as a function of axial rotation (γ).

(to the left) is possible by increasing muscle force FTRR and decreasing force FTRL, see Fig. 9. Their sum is almost constant and in the vertical direction. The point of attachment of the m. trapezius PO moves to the right. Only little force of the sternocleidomastoid muscle is needed to balance the head. When $\gamma = 35°$ the line of action of FTRR is almost vertical and further rotation is not possible only by altering FTRL and FTRR. For greater rotations the right sternocleidomastoid muscle is needed. However, the direction of the line of action of this muscle is very unfavourable to achieve axial rotation of the head. Action of the left sternocleidomastoid muscle is needed to balance the head in the frontal plane, causing the joint reaction forces to increase fast. Besides, the m. trapezius, which is necessary to equilibriate the head in the sagittal plane, gives a moment which opposes further rotation, see Fig. 9.

Similar to Fig. 8, Fig. 10 shows the joint reaction forces and muscle forces during lateral flexion. As expected, the m. sternocleidomastoideus must be active. Due to the dorsal position of SL and SR with respect to point B (see Fig. 4a), the m. sternocleidomastoideus also gives a moment on the y-axis. This moment relieves the m. trapezius. For lateroflexion of more than 16° this moment becomes so great that action of m. rectus capitus is needed to prevent the head from rotating backward.

4. DISCUSSION

Before drawing conclusions, it must be emphasized that the model is a simplification of reality and that reliable anthropometric data hardly exist. Some calculated forces can be compared with data in the literature. Rizzi and Covelli (1975a, b) calculated the force of the m. trapezius in the neutral position and, in

extreme flexion, they found for the sum of the left and right muscle 19 and 39 N. Less and Eickelberg (1976) estimated the neck muscle force for two positions between neutral position and extreme flexion as 24 and 41 N. The forces calculated by the model are 26 and 36 N, these values are of the same order of magnitude.

An indication of a correct proportion of forces follows from considering the joint reaction forces on the levels C_2-C_3 and C_7-T_1 in relation to the area of the intervertebral discs. The ratio of these areas is circa 1:2.5, which is consonant to the ratio of the forces FK:FR. The mean ratio in various positions of the head is 1:2.4, see Table 1.

A sensitivity analysis was performed to determine which parameters affected the results the most. In the neutral position and in the extreme positions all parameters were varied one by one up to a deviation of 10%. A parameter was considered to be critical when its influence on the results was more than 10%. As expected, the geometric data in the neutral position turned out to be the most critical. Varying the parameter φ_0 caused the joint reaction force FR to deviate as much as 25%. This same force showed a deviation of 60% when all parameters were given a deviation of 10%. So the model turned out to be rather sensitive for geometric data, emphasizing the importance of reliable anthropometric data.

The optimization algorithm leads to the minimal joint reaction forces. Synergistic muscle forces and muscle forces for stabilization are not incorporated into the model. Due to the fact that in vivo measurements of muscle forces are impossible, the choice for an optimization criterion only can be made by intuitively reasonable assumptions. The field of interest for this study concerns F-16 flight situations where neck loads occur which cause vertebrae to fail. Especially in these situations, the criterion of least possible joint reaction force seems reasonable. Both muscle action for stabilization and other strategies to obtain equilibrium will increase these reaction forces. The estimation of joint reaction forces by this model will be a conservative one, in reality the joint reaction forces may be greater. A number of optimization techniques for knee flexion was compared by Dul et al. (1984).
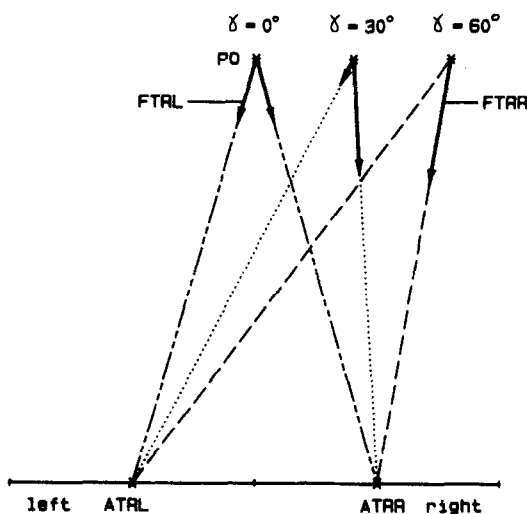

Fig. 9. Back view on the m. trapezius. Distribution of muscle force over left and right trapezius muscle during various stages of axial rotation (graph not to scale).

Table 1. Ratio between FK and FR in different situations, spread over the range of motion of α, β and γ

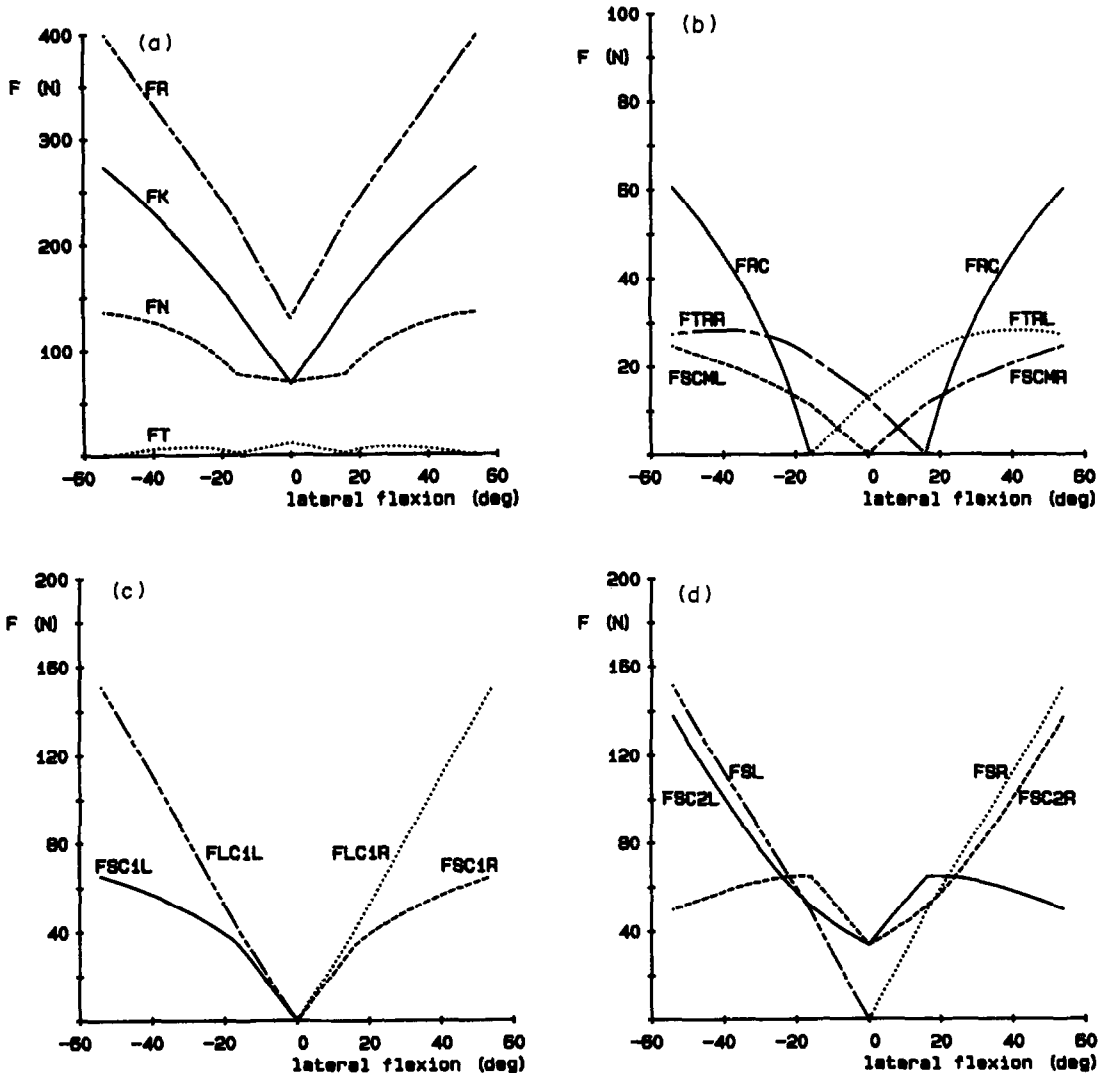|	FK	FR	FK:FR
Neutral	68	130	1:1.9
$\alpha = 25°$	178	274	1:1.5
$\alpha = 50°$	262	402	1:1.5
$\beta = 40°$	80	287	1:3.6
$\beta = -40°$	38	98	1:2.6
$\beta = -80°$	54	315	1:5.8
$\gamma = 25°$	80	136	1:1.7
$\gamma = 50°$	136	231	1:1.7
$\gamma = 75°$	260	260	1:1.4

Fig. 10a, b, c, d. Joint reaction forces and muscle forces as a function of lateral flexion (α).

5. CONCLUSIONS

With the help of the described neck model, muscle forces and joint reaction forces in the neck can be estimated in various situations. Although it is difficult to verify the model as far as demonstrating real existing forces is concerned, we obtained indications that the order of magnitude is correct. So the approach followed leads to results, be it of limited accuracy. The most reliable conclusions can be drawn with respect to comparing different situations.

During flexion, especially, the joint reaction force on C_7-T_1 and the force on ligamentum transversum atlantis increase. The joint reaction forces are minimal in a situation of backward flexion (30° for FR, 55° for FN and FK). From a biomechanical point of view this is a favourable situation, but not comfortable for physiological reasons. In normal situations the trapezius muscle is active, therefore this muscle must be

relatively strong. During axial rotation of less than 35°, only small changes in muscle force and joint reaction force appear. From 35° these forces increase very fast. A possible example of this fact can be seen by people in a meeting who move their chair when they have to look aside for a long time.

Muscle forces and joint reaction forces (except FT) also increase rapidly during lateral flexion, making these situations uncomfortable. However, in daily life, situations in which people are forced into lateral flexion for a sustained amount of time are not common.

REFERENCES

Aghina, J. C. F. M. (1984) Cervicale klachten bij jachtvliegers. IGDKLu, Soesterberg (internal report, in Dutch).
Dul, J., Snijders, C. J. and Timmerman, P. (1982) Bewegungen und Kräfte im oberen Kopfkelenk beim Vorbeugen der Halswirbelsäule. Manuelle Medizin 20, 51–58.

Dul, J., Townsend, M. A., Shiavi, R. and Johnson, G. E. (1984) Muscular synergism—I. On criteria for load sharing between synergistic muscles. *J. Biomechanics* **17**, 663–667.

Glaister, D. H. (1987) The effects of off-axis loading on head mobility. *Proceedings Air Crew Helmets and Helmet Mounted Devices*, Royal Aeronautical Society, London, 10 Feb, 13.1–13.4. Hauts GU 14–6SZ, U.K.

Graef, P. de and Ingels, M. (1982) Het optreden van cervicalgien bij piloten onderworpen aan langdurig aangehouden positieve versnellingen. *Acta. Med. Mil. Belg.* **134**, 115–119.

Kazarian, L. E., Belk, W. F. and Hoffman, H. P. (1979) Traumatic lesions of the cervical spine 1971–1979. Agardograph/AMRL-TR-80-53.

Kiss, F. and Szentágothai, J. (1964) *Atlas of Human Anatomy*, Vol. 1. Pergamon Press, Oxford.

Lanz, T. von and Wachsmuth, W. (1955) *Praktische Anatomy (Teil Hals)*. Springer, Berlin.

Less, M. and Eickelberg, W. W. B. (1976) Force changes in neck vertebrae and muscles. In *Biomechanics V-A* (Edited by Komi, P. V.). University Park Press, Baltimore.

McElhaney, J. H., Doherty, B. J., Paver, J. G., Myers, B. S. and Grey, L. (1989) Flexion, extension and lateral bending responses of the cervical spine. *Proceedings 67th Aerospace Medical Panel Meeting*, Agard, Munchen.

Miller, J., Schultz, A., Warwick, D and Spencer, D. (1986) Mechanical properties of lumbar spine motion segments under large loads. *J. Biomechanics* **19**, 79–84.

Penning, L. (1978) Normal movements of the cervical spine. *Am. J. Roentgenol.* **130**, 317–326.

Petrofsky, J. S. and Phillips, C. A. (1982) The strength-endurance relationship in skeletal muscle: its application to helmet design. *Aviation Space Envir. Med.* **53**, 365–369.

Phillips, C. A. and Petrofsky, J. S. (1983) Neck muscle loading and fatigue: systematic variation of headgear weight and centre-of-gravity. *Aviation Space Envir. Med.* **54**, 901–905.

Rieck, A. (1981) To the fundamentals of the isometric muscle training as a physical counteraction of the jet pilot against 'G'-loads. *Air Crew Safety and Survivability*, AGARD, 1–6.

Rizzi, M. A. and Covelli, B. (1975a) Die Funktion der Nackenmuskulatur biomechanisch berechnet. *Manuelle Medizin* **13**, 101–106.

Rizzi, M. A. and Covelli, B. (1975b) Biomechanischer Beitrag zur Berechnung der Kräfte der Halsmuskulatur und deren Wirkung. *Z. Orthop.* **113**, 371–377.

Romanes, G. J. (1981) *Cunningham's Textbook of Anatomy*. Oxford University Press, Oxford.

Schulz, A. B., Andersson, G. B. J., Haderspeck, K., Örtengren, R., Nordin, M. and Björk, R. (1982b) Analysis and measurements of lumbar trunk loads in tasks involving bends and twists. *J. Biomechanics*, **15**, 669–675.

Schulz, A., Andersson, G., Örtengren, R., Haderspeck, K. and Nachemson, A. (1982a) Loads on the lumbar spine: validation of a biomechanical analysis by measurements of intradiscal pressures and myoelectric signals. *J. Bone Jt Surg.* **64**, 713–720.

Shirazi-Adl, S. A., Ahmed, A. M. and Shrivastava, S. C. (1986) A finite-element study of a lumbar motion segment subjected to pure sagittal plane moments. *J. Biomechanics* **19**, 331–350.

Wells, K. F. (1971) *Kinesiology*. W. B. Saunders, Philadelphia.

White, A. A. and Panjabi, M. M. (1978) *Clinical Biomechanics of the Spine*. J. B. Lippincott, Philadelphia.

Williams, M. and Lissner, H. R. (1962) *Biomechanics of Human Motion*. W. B. Saunders, Philadelphia.

APPENDIX A

List of points in model:

E	centre of rotation C_2–C_3 flexion–extension and lateral flexion
D	centre of axial rotation C_1–C_2
C	centre of rotation C_1–C_2 flexion–extension
B	centre of rotation C_0–C_1 flexion–extension
A	centre of rotation C_0–C_1 lateral flexion
TC	top clivus, centre of gravity head

Table 2. Position of points in neutral position

Point	x	y (mm)	z	Point	x	y (mm)	z
E	35	0	98	C2VL	45	17	94
D	35	0	125	C2VR	45	−17	94
C	35	0	133	C2VM	45	0	94
B	29	0	146	C2DL	26	20	101
A	22	0	162	C2DR	26	−20	101
TC	71	0	162				
PB	52	0	166	ATRL	−40	50	0
PO	−48	0	167	ATRR	−40	−50	0
SL	−0.8	60	146	ASCL	80	5	0
SR	−0.8	−60	146	ASCR	80	−5	0
				ALC	15	0	0
C1V	50	0	137	ASPL	−40	0	0
C1M	45	0	135	ASPR	−40	0	0
C1DL	16	5	127	ASL	15	75	0
C1DR	16	−5	127	ASR	15	−75	0

Table 3. List of muscles incorporated into the model

Abbreviation	Points of attachment	Name of muscle
FTRL	PO-ATRL	m. trapezius left
FTRR	PO-ATRR	m. trapezius right
FSCM	SL-ASCL	m. sternocleidomastoid left
FSCMR	SR-ASCR	m. sternocleidomastoid right
FSC1L	C1DL-C2DL	m. splenius cervicis left
FC1R	C1DR-C2DR	m. splenius cervicis right
FLC1L	C1V-C2VL	m. longus colli left
FLC1R	C1V-C2VR	m. longus colli right
FSC2L	C2DL-ASPL	m. splenius cervicis left
FSC2R	C2DR-ASPR	m. splenius cervicis right
FLC	C2VM-ALC	m. longus colli
FSL	C2DL-ASL	m. scaleni left
FSR	C2DR-ASR	m. scaleni right

PB	pars basilaris
PO	protuberance occipitalis
SL	proc. mastoideus left
SR	proc. mastoideus right
C1V	ventral side atlas
C1M	massa lateralis atlas
C1DL	dorsal side atlas left
C1DR	dorsal side atlas right
C2VL	ventral side C_2 left (tuberculum anterius)
C2VR	ventral side C_2 right
C2VM	ventral side C_2 middle
C2DL	dorsal side C_2 left
C2DR	dorsal side C_2 right
ATRL	intersection in x–y plane line of action m. trapezius left
ATRR	intersection in x–y plane line of action m. trapezius right
ASCL	intersection in x–y plane line of action m. sternocleidomastoideus left
ASCR	intersection in x–y plane line of action m. sternocleidomastoideus right
ALC	intersection in x–y plane line of action m. longus colli
ASPL	intersection in x–y plane line of action m. splenius cervicis left
ASPR	intersection in x–y plane line of action m. splenius cervicis right
ASL	intersection in x–y plane line of action m. scaleni left
ASR	intersection in x–y plane line of action m. scaleni right

APPENDIX B

In this appendix the calculation of the equilibrium of a fictitious link is given in an arbitrary position (see Fig. A1). The points D, L and R are defined as points of attachment of muscles on this link. The lines of action for the muscles are drawn as dashed lines. The points DD, LL and RR are the intersections of the lines of action in the x–y plane. Point M is the centre of rotation.

The input parameter is a known force FG with components FG_x, FG_y and FG_z acting on point V. The moment of this force on point M is given by the equation:

$$MG = FG \times (V - M). \qquad (A1)$$

This moment vector has three components, their magnitudes are called MG_x, MG_y and MG_z. The joint reaction force FM, which has three independent components FM_x, FM_y and FM_z, acts on point M, so it has no moment on this point.

The direction of lines of action of the muscles are defined by D-DD, L-LL and R-RR. The muscle force vector F1, corresponding with the first line of action, can be written as:

$$F1 = K_1 * \frac{(D - DD)}{|D - DD|}. \qquad (A2)$$

K_1 is a scalar, representing the magnitude of this muscle force, the quotient is a unit vector in the direction of this
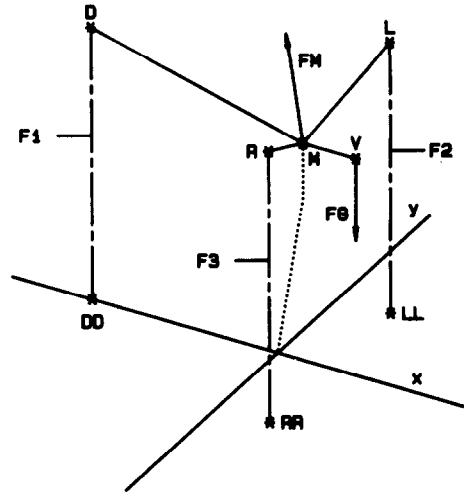

Fig. A1. A fictitious link in equilibrium with one joint, three muscle forces and an external load.

force. This unit vector can be written as DU, so equation (A2) can be rewritten as:

$$F1 = K_1 * DU. \qquad (A3)$$

In the same way the muscle forces F2 and F3 can be defined as:

$$F2 = K_2 * LU \qquad (A4)$$

$$F3 = K_3 * RU. \qquad (A5)$$

The moment M1 of F1 on point M can be written as:

$$M1 = F1 \times (D - M), \qquad (A6)$$

or, using equation (A3):

$$M1 = K_1 * DU \times (D - M). \qquad (A7)$$

Equation (A7) can be abbreviated to:

$$M1 = K_1 * DP. \qquad (A8)$$

In the same way the moments M2 and M3 can be written as:

$$M2 = K_2 * LP, \qquad (A9)$$

$$M3 = K_3 * RP. \qquad (A10)$$

The equations which describe the equilibrium are:

$$F1 + F2 + F3 + FM_x + FM_y + FM_z = -FG, \qquad (A11)$$

$$M1 + M2 + M3 = -MG, \qquad (A12)$$

or, in matrix notation:

$$\begin{bmatrix} DU_x & LU_x & RU_x & 1 & 0 & 0 \\ DU_y & LU_y & RU_y & 0 & 1 & 0 \\ DU_z & LU_z & RU_z & 0 & 0 & 1 \\ DP_x & LP_x & RP_x & 0 & 0 & 0 \\ DP_y & LP_y & RP_y & 0 & 0 & 0 \\ DP_z & LP_z & RP_z & 0 & 0 & 0 \end{bmatrix} * \begin{bmatrix} K_1 \\ K_2 \\ K_3 \\ FM_x \\ FM_y \\ FM_z \end{bmatrix} = \begin{bmatrix} -FG_x \\ -FG_y \\ -FG_z \\ -MG_x \\ -MG_y \\ -MG_z \end{bmatrix}.$$

The matrix is filled with geometrical data, the right term represents the load. The muscle forces K_1, K_2, K_3 and the components of the joint reaction force can be determined by solving this system.